ADVANCED MATERIALS TECHNOLOGIES
www.advmattechnol.de

All-Textile Triboelectric Generator Compatible with Traditional Textile Process

*Lushuai Zhang, Yanhao Yu, Gregory P. Eyer, Guoquan Suo, Liz Anna Kozik, Marianne Fairbanks, Xudong Wang, and Trisha L. Andrew**

All-textile triboelectric generators (TEGs) allow for seamless integration of TEGs into garments, while maintaining the intrinsic flexibility, breathability, durability, and aesthetic value of normal textiles. However, practical approaches to construct fabric TEGs using traditional textile processes, such as sewing, weaving, and knitting, are underreported. In this work, two approaches to create an all-textile TEG using straight-forward textile manufacturing methods are presented. The first approach is to assemble two different cloths of opposite surface charge characteristics in a face-to-face configuration. A cotton fabric functionalized with fluoroalkylated polymeric siloxanes is necessary to generate usable triboelectric power output, when coupled with a pristine nylon cloth. The increased surface charge density by introducing fluoroalkyl groups is confirmed by Kelvin probe force microscopy measurements. The second approach is to weave or knit together two different conductive threads of opposite surface charge characteristics to create a monolithic triboelectric textile. The weave or knit pattern used to assemble this textile directly controls the density of contact points between the two types of threads, which, ultimately, determines the areal triboelectric power output of the textile. Overall, two feasible methods for constructing unprecedented textile-based triboelectric generators with notable power output are presented.

1. Introduction

The collective energy consumption of rapidly growing low-power electronic devices is intimidating. Take one iPhone model sold globally over one year as an example: the collective electricity consumed by these units is equivalent to that of over fifty thousand US households. As of 2016, 1 billion people worldwide are estimated to own smartphones. In addition to smartphones, wearable devices are predicted to expand from the realm of fitness and medical products to glasses and watches, with 80 million units shipped in 2015, and over 200 million units estimated to be shipped in 2019. All these devices together put a massive burden on energy consumption. However, the low-power advantage of each single device renders self-sustaining power supplies possible. Charging low-power electronics by ambient energy-harvesting technologies not only relieves them from bulky batteries, but also lays a foundation of sustainable development on this relatively new market in terms of minimum use of fossil fuels.

Energy resources that can be converted into electric power include solar, electromagnetic radiation, thermal, and mechanical energy.[1–4] Each energy resource has its own advantages in particular environments. Triboelectric generators (TEGs) are a nascent technology, notable for scavenging energy released by small body motions.[4–6] The principle of TEGs is based on charge collection from ubiquitous contact electrification and electrostatic induction. Upon the physical contact of two dissimilar materials (mostly polymers), electrostatic charge will be generated on the triboelectric polymer surface, either by ion transfer or electron transfer.[7,8] This surface charge density will be stabilized after several cycles of contact and separation. Subsequent electrical outputs (e.g., open circuit voltage and short circuit current) linearly depend on the surface charge density.[9] Great progress has been made to achieve TEGs with high electrical output by optimizing micro- and nanoscale morphology,[10,11] surface chemistry,[12] and device architecture.[13]

One highly attractive and practical approach to harness triboelectric power generation is to create TEG-incorporated garments capable of constantly harvesting body motion energy. Ideally, such smart garments will serve as wearable power supplies for low-power electronics. A remaining question is how best to incorporate these devices into garments while simultaneously retaining the comfort and aesthetic qualities of common apparel, which are important factors that can lead to widespread technology adoption and proliferation. Some research endeavors were aimed at polydimethylsiloxane (PDMS)/textile composites[14–17] and woven fabric bands.[18–20] The use of PDMS introduces problems, such as mitigating the inherent

Dr. L. Zhang, Y. Yu, G. Suo, Prof. X. Wang, Prof. T. L. Andrew
Department of Materials Science and Engineering
University of Wisconsin-Madison
Madison, WI 53706, USA
E-mail: tlandrew@wisc.edu
G. P. Eyer
Department of Chemistry
University of Wisconsin-Madison
Madison, WI 53706, USA
L. A. Kozik, Prof. M. Fairbanks
Textiles and Fashion Design Studies
School of Human Ecology
University of Wisconsin-Madison
Madison, WI 53706, USA

DOI: 10.1002/admt.201600147

flexibility and breathability of textiles and compromising durability and washability. What is more hurtful is that textiles have natural roughness and a high density of chemically diverse functional groups on their surfaces, which can, if harnessed properly, lead to high surface charge density in TEGs. These natural advantages of textile surfaces are completely overlooked when PDMS composites are created with textiles, and costly postfabrication processes would be required if similar roughness and functional group density were to be introduced on PDMS surfaces. In contrast, preliminary reports of hand-woven all-fabric TEGs demonstrated the feasibility of creating wearable TEGs using traditional textile manufacturing processes; however, this idea has not yet been successfully married with the fast, large-area textile production methods available today, such as sewing, loom-weaving, and knitting. Integrating TEG device fabrication with these longstanding textile processes will be integral to creating cost-effective triboelectric garments capable of powering common consumer electronic devices.

Herein, we report two approaches to create wearable, all-textile triboelectric generators using traditional textile manufacturing processes. In the first approach, we capitalize on the natural triboelectric properties of common fabrics and simple silanization chemistry to effect usable triboelectric power generation in a sewn sample. Silanization was observed to significantly enhance power output due to higher surface charge density, as confirmed by Kelvin probe force microscopy measurements. In the second approach, we create a triboelectric textile swatch by weaving or knitting together two different conductive threads in a simple a two-in-one pattern. The knitted structure was found to both increase the contact area between electron donor and acceptor components of the TEG and to provide additional friction sites that lead to an unprecedented strategy to increase triboelectric power output.

2. Results and Discussion

First, an all-fabric TEG was constructed by sewing together different fabrics. Nylon, which is composed of poly(amide) fibers, is a strong positive triboelectric material. Cotton, which is composed of cellulose fibers (**Figure 1**a), is a weak, ambipolar triboelectric material, with natural surface charge characteristics that place cotton in the middle of the triboelectric series. However, the hydroxyl groups in cellulose are capable of reacting with chlorosilanes to form various surface-grafted siloxanes and, therefore, cotton cloths can be chemically functionalized using commercial silanes to tune their triboelectric properties.

A cotton textile was successfully functionalized with trichloro(1*H*,1*H*,2*H*,2*H*-perfluorooctyl)silane to transform normally neutral cotton fabrics into a strong negative triboelectric material (F-cotton). Due to the silanization conditions employed, a polymeric fluoroalkylated siloxane film was likely grafted onto the cotton fabrics (Figure 1a).[21] Scanning electron microscope (SEM) images of the cotton fabrics before and after silanization reveal the presence of a conformal coating on each cotton fiber: the surface of the pristine cotton sample is full of wrinkles, while the functionalized cotton sample displays a smoother surface. Successful silane functionalization was further confirmed using X-ray photoelectron spectroscopy (XPS, Figure 1b). XPS scans of pristine cotton cloths display an intense C 1S peak at 284.8 eV and an O 1S peak at 533.08 eV. Upon surface grafting with fluoroalkylated siloxane films, a F 1S peak at 689.08 eV dominates the XPS scan. Moreover, the C 1S peak splits into two peaks. The lower binding energy peak at 284.8 eV is mainly from the cotton, and the higher binding energy peak at 290.1 eV can be attributed to fluorine-attached carbon atoms.

The stability of the grafted polymeric fluoroalkylated siloxane films on cotton cloths was tested by extensive sonication experiments and water contact angle measurements. Figure 1a shows the hydrophilicity of a pristine cotton (left) and hydrophobicity of a fluoroalkylated siloxane-grafted cotton (F-cotton) (right). The water droplet contact angle for the pristine cotton cloths is close to zero degrees, since cotton is highly hydrophilic. Upon functionalization with a fluoroalkylated siloxane, the cotton cloth is rendered hydrophobic. This hydrophobicity is retained after 30 min of continuous sonication, implying that the grafted siloxane films created upon silane functionalization are chemically stable and robust. Such stability is of particular importance for TEGs because the power output relies on surface, not bulk, charges.

Figure 2a shows an optical image of an all-textile TEG created by sewing together a nylon cloth or an F-cotton cloth and

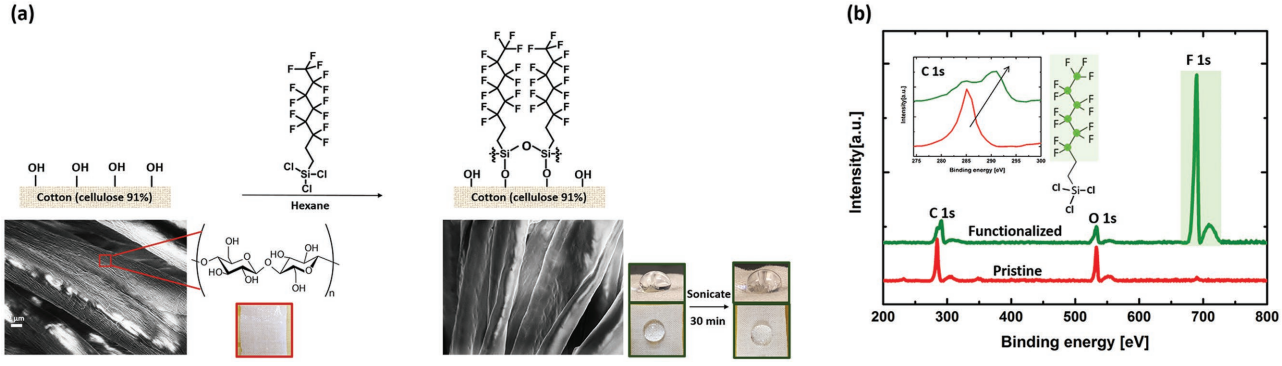

Figure 1. a) Schematic showing the functionalization of cotton textiles with trichloro(1*H*,1*H*,2*H*,2*H*-perfluorooctyl)silane, SEM images of cotton textiles before (left) and after (right) functionalization, and optical images of cotton textile with water dropped on surface. The pristine sample is highly hydrophilic and the functionalized cotton fabric is hydrophobic. The stability of the covalently bonded film is confirmed by sonicating the functionalized cotton sample in water for 30 min. b) XPS scans of the pristine (red) and functionalized (green) cotton cloth.

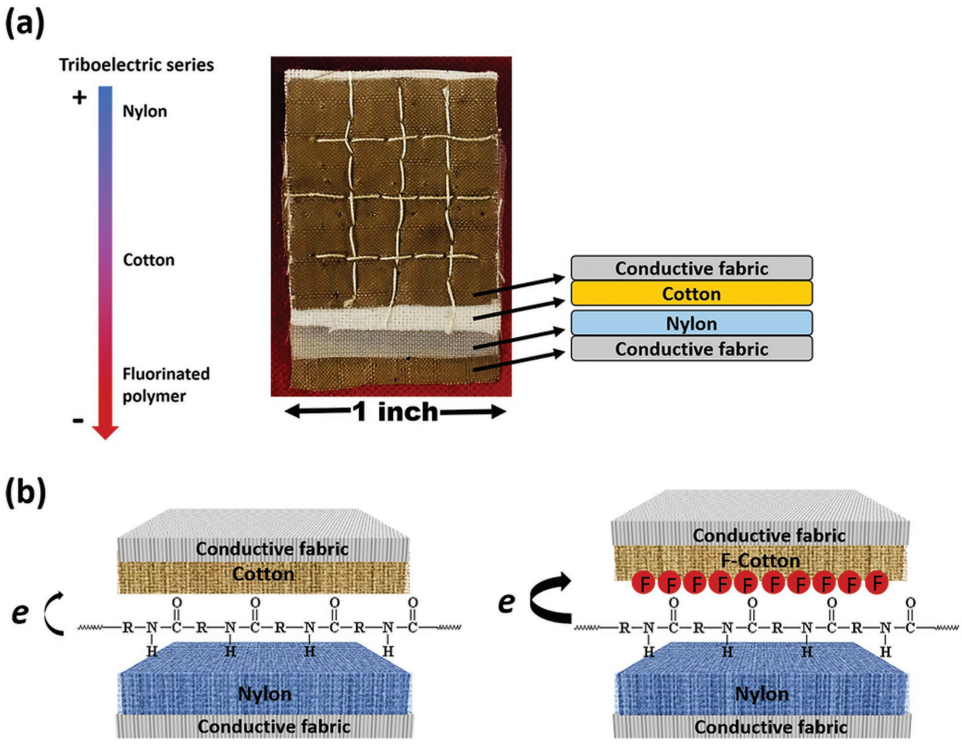

Figure 2. a) Triboelectric series and optical image of an all-textile TEG comprised of cotton/conductive fabric and nylon/conductive fabric. b) Schematic illustration of a control textile TEG textile comprised of cotton/conductive fabric and nylon/conductive fabric (left) and a textile TEG comprised of F-cotton/conductive fabric and nylon/conductive fabric (right). Cotton or nylon textiles are tightly attached to conductive fabrics by sewing.

a silver-coated nylon cloth, respectively. In this all-textile TEG, nylon serves as the positive triboelectric material, F-cotton serves as the negative triboelectric material, and silver-coated nylon functions as the electrode. The two triboelectric cloths were tightly sewed to the silver-coated nylon cloth electrodes using regular cotton thread to achieve good contact for efficient charge collection. Figure 2a shows a schematic illustration of this TEG device operating in contact-separation mode and a schematic of the control device created with pristine, unfunctionalized cotton instead of F-cotton. Nylon is on the top of the triboelectric series, with the strongest tendency be positively charged during contact electrification. Fluorinated materials are easily negatively charged upon contact electrification and are on the bottom of the triboelectric series. Pristine cotton is in the middle of the triboelectric series. Based on the triboelectric series, a moderate amount of surface charge can be expected with the nylon/cotton pair, while maximum surface charge density can be achieved with the nylon/F-cotton pair.

Kelvin probe force microscopy (KPFM) was used to examine the relative charge density on nylon surfaces before and after contact electrification with cotton or F-cotton. KPFM is primarily used to study the electronic properties of conductors and semiconductors, but it is also successfully applied to detect charge distributions on insulating surfaces.[22] Figure S1a–c (Supporting Information) shows the topography (top row) and contact potential difference (CPD) (bottom row) images obtained for pristine nylon textiles before friction, after friction against pristine cotton, and after friction against F-cotton, respectively. Each topography image shows the rough surface expected for a nylon fabric. All three scans of the various nylon fabrics before and after friction were conducted using the same KPFM tip, and thus the relative differences in CPD values between the three samples directly reflects the variation in surface charge density of the different nylon fibers. A more positive CPD value represents a higher negative charge density or a lower positive charge density on the surface. Under the same scale region of −1.7 to 1 eV, significant differences in surface potential exist between the three nylon samples. The nylon textile before friction has the highest potential with an average value of 0.6 V. After friction against pristine cotton, the CPD is dramatically decreased to −0.2 V, a −0.8 V change. This CPD change can be attributed to the loss (gain) of negative (positive) charges on the nylon surface upon contact electrification with pristine cotton. After contact with F-cotton, the CPD is decreased to −1.1 V, indicating greater contact electrification than against pristine cotton. This observation supports the utility of silane treating cotton, which augments charge transfer between nylon and cotton upon contact electrification and should, therefore, lead to increased power output in a triboelectric device.

The mechanism of contact electrification resulting from the physical contact of two dissimilar materials is still unclear. Proposed mechanisms include ion transfer and electron transfer upon contact. Although an ion transfer model is preferred for insulators by many researchers,[7] electron transfer was observed between poly(methyl methacrylate) and poly(tetrafluoroethylene) (PTFE).[8] The mechanism of the charge transfer process between nylon and F-cotton was

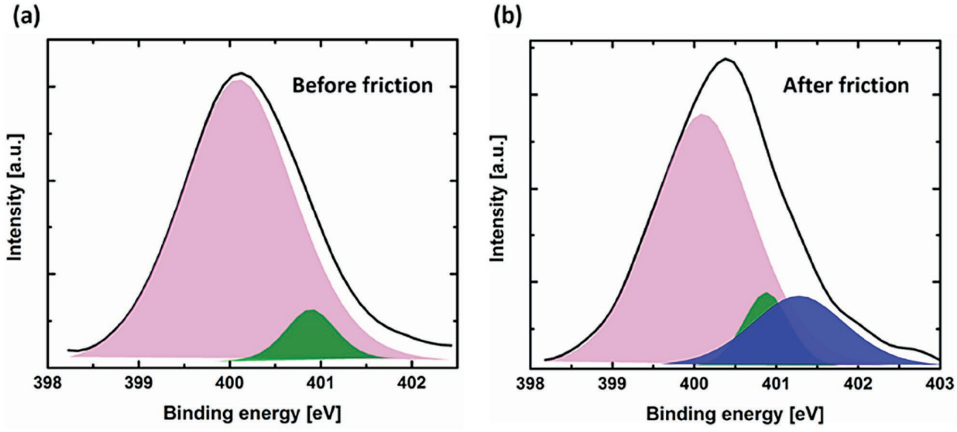

Figure 3. XPS high resolution scan of N 1S of nylon a) without friction and b) after friction against F-cotton.

studied using XPS and electron paramagnetic spectroscopy (EPR). In particular, the XPS signal originating from the core electrons of the nitrogen atoms in nylon were closely examined. **Figure 3** shows the high resolution XPS scan of the nitrogen core electrons in nylon before (Figure 3a) and after (Figure 3b) contact with F-cotton, respectively. In Figure 3a, there are two nitrogen peaks: one at 400.1 eV with a full width at half maximum (FWHM) of 1.5 eV, and one at 400.8 eV with a FWHM of 0.7 eV. After friction with F-cotton, a new peak arises at 401.3 eV with a FWHM of 1.37 eV. A shift to higher binding energy was previously attributed to cationic nitrogen (N^+) as opposed to neutral N in polyaniline.[23] Therefore, the new peak at higher binding energy that is observed upon friction with F-cotton was tentatively ascribed to the formation of a cationic nitrogen in nylon that is formed as a result of electron transfer from nylon to F-cotton. If this electron transfer were indeed occurring, a poly(amide) radical cation would be left behind in the nylon, which should be detectable via EPR if it is paramagnetic. Indeed, a new EPR peak at 3475–3480 Gauss is observed to evolve upon rubbing a nylon sample with cotton (see Figure S2, Supporting Information) that is tentatively ascribed to a poly(amide) radical cation. Further, this new peak persists in the EPR spectrum of rubbed nylon cloths for upto 20 min, indicating that the cationic unpaired electron species formed in nylon upon rubbing with cotton is stable.

Figure 4 illustrates the operative sequence followed for generating power from the all-textile TEG described above. Figure 4a shows the open circuit condition, and Figure 4b displays the short circuit condition. Under open circuit conditions, no charge transfers between the two electrodes. The predicted open circuit voltage (V_{oc}) is linearly proportional to the surface charge density as shown in Equation (1),[9] where σ is the surface charge density, $x(t)$ is the instantaneous distance between the two materials, and ε_0 is the permittivity of vacuum

$$V_{oc} = \frac{\sigma x(t)}{\varepsilon_0} \tag{1}$$

$$J_{sc} = \frac{\sigma d_0}{(d_0 + x(t))^2} \frac{dx}{dt} \left(d_0 = \frac{d_1}{\varepsilon_{r1}} + \frac{d_2}{\varepsilon_{r2}} \right) \tag{2}$$

Under short circuit conditions, when cotton and nylon are physically separated from one another, the electric field between the two textiles electrostatically induces a current to flow between the two electrodes through an external circuit, generating a short circuit current density J_{sc} as shown in Equation (2),[9] where σ is surface charge density, $x(t)$ is the instantaneous distance between the two materials, ε_0 is the vacuum permittivity, d_1 and d_2 are thickness of the two dielectric materials, respectively, and ε_{r1} and ε_{r2} are relative permittivity of the two dielectric materials. The current is also generated from the fully released state to the pressed state.

Equations (1) and (2) reveal that surface charge density is an efficient tool to tune V_{oc} and J_{sc} simultaneously. Additionally, the effective thickness d_0 is another parameter determining J_{sc}. The small thickness and large dielectric constant of fabrics give rise to smaller d_0 values, which effectively increases J_{sc}. Further, there is a large range of available textile thicknesses, from tens of micrometers to a few millimeters, providing extra room to enhance J_{sc}.

In this work, the cotton cloth is 290 µm thick and the nylon cloth is 100 µm thick. As shown in Figure 4a, the V_{oc} of the textile TEG with pristine cotton is 1.5 V, and that of the TEG with F-cotton is 8 V. An increase of more than fivefold is obtained as a consequence of the increased surface charge density achieved upon functionalizing cotton with a fluoroalkylated polysiloxane. As shown in Figure 4b, J_{sc} is also increased by threefold from 0.3 µA cm^{-2} with pristine cotton to 1 µA cm^{-2} with F-cotton. The magnitude of transferred charge is also increased by threefold from 10 to 30 µQ m^{-2}. Thus, by using appropriate surface chemical modifications, an all-textile TEG composed of two cloths pressed together in a face-to-face configuration can be easily assembled by a simple sewing process, which generates notable power output.

For practical use, the output power for a load depends on the resistance of the load. The output voltage and current dependence of a working TEG device containing surface functionalized cotton fabric on the external loads was tested. The loads were varied from 1.5 to 1000 MΩ, as shown in Figure 4c. As load resistance is increased, the voltage rises and is saturated at a value of 120 V, while the current decreases due to the ohmic loss. As shown in Figure 4c, the

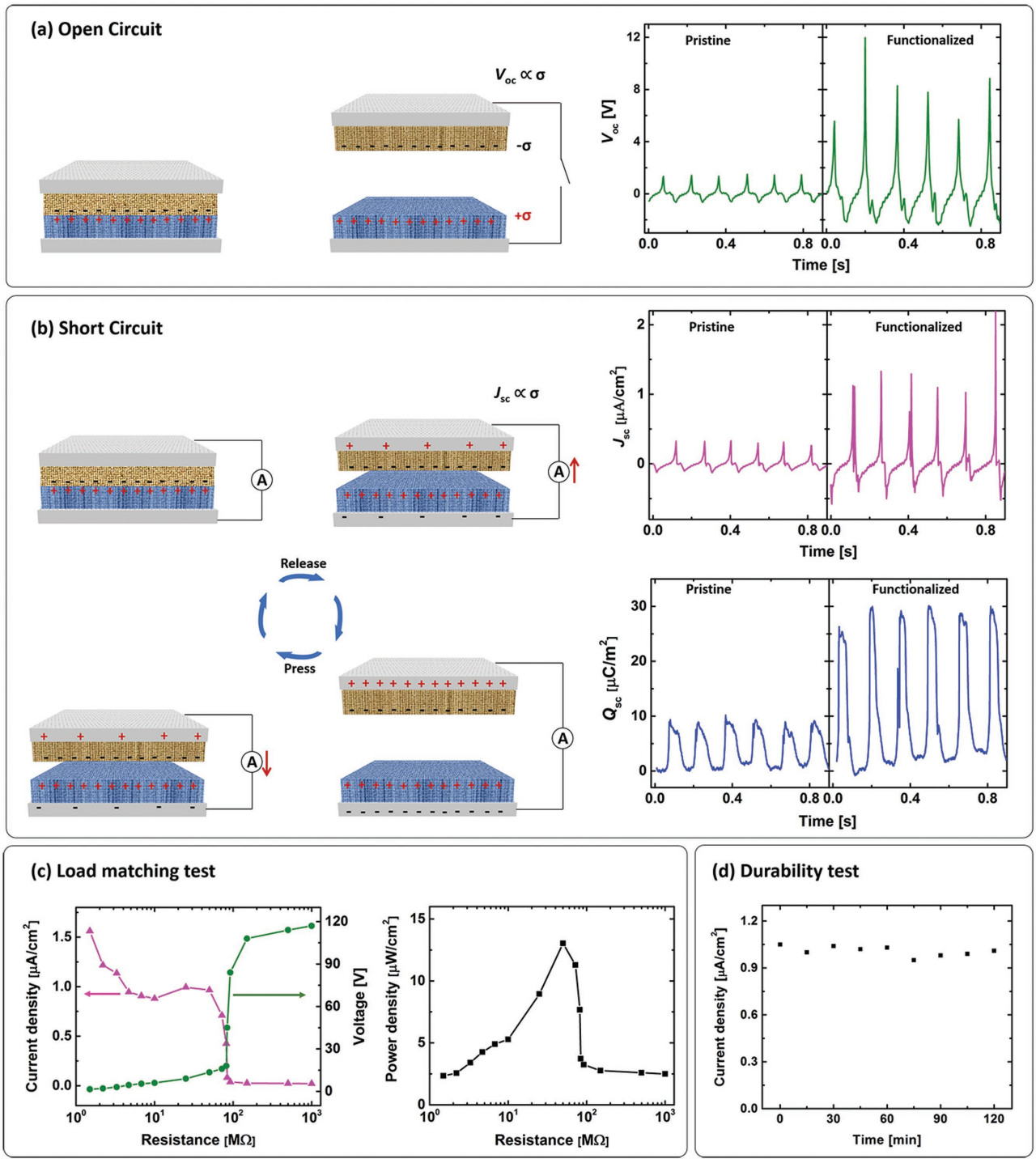

Figure 4. Schematic illustration and electric output measurements under a) open circuit condition and b) short circuit condition for an all-textile TEG created by sewing together nylon and functionalized cotton cloths in a face-to-face configuration. c) Dependence of output voltage, current, and instantaneous power on load resistance of TEG device containing surface functionalized cotton. d) Durability test of TEG device containing surface functionalized cotton.

instantaneous power on the load reached a maximum value of 13 μW cm^{-2} at a load resistance of 50 MΩ. The durability test displayed in Figure 4d reals the stability of the TEG device with surface functionalized cotton under continuous operation for 2 h.

A second type of triboelectric textile was created by weaving or knitting together two different conductive threads in a simple a two-in-one pattern. Two-in-one textile TEGs are defined as a single fabric containing threads of both charge donor and acceptor materials that are woven or knitted together into one monolithic cloth.

Such two-in-one textile TEGs are attractive because they do not require two separate parts, which allows for easier and straightforward integration into arbitrary parts of garments.

Figure 5a illustrates the approach taken to create two-in-one triboelectric textiles. Conductive silver-plated nylon threads were used to serve as both the positive triboelectric material and charge collector. The same conductive nylon thread was wrapped with commercially available PTFE tape and this PTFE-wrapped thread was used as the negative triboelectric material.

Figure 5b shows the optical images of two woven (Weave 1 and Weave 2) and one knitted triboelectric textile (Knit 1). Next to the optical images are schematic illustrations of the weave or knit pattern employed to create each triboelectric textile. The PTFE wrapped thread is defined as the weft (latitude in Weave 1 and longitude in Weave 2), and the naked silver-coated nylon thread is defined as the warp. The weave pattern of sample Weave 1 is of higher density, with 32 weft segments (1 in. in length) and 20 warp (2 in. in length) threads. The weave pattern

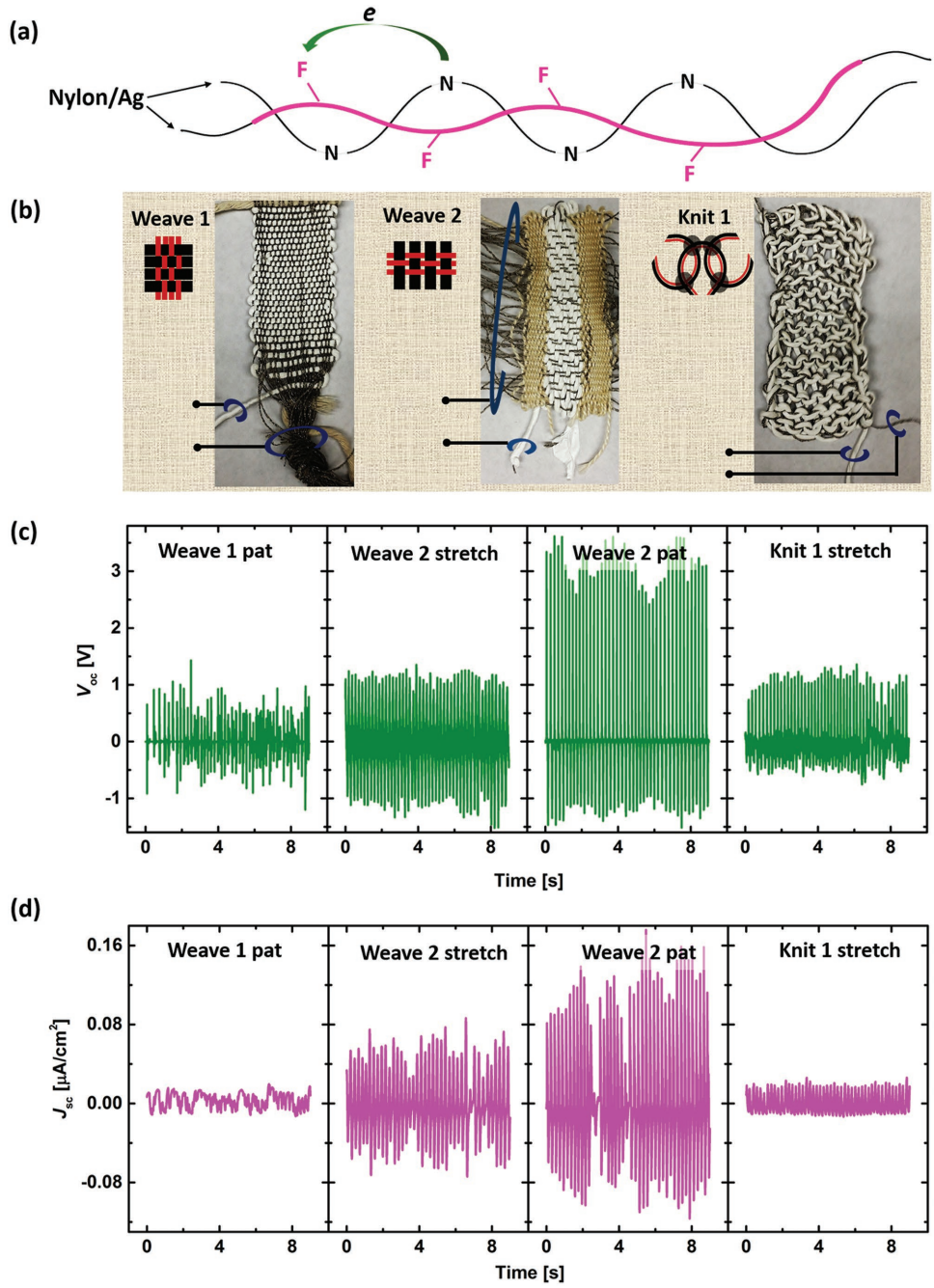

Figure 5. a) Schematic illustration of a two-in-one triboelectric textile comprised of a silver/nylon conductive thread and a PTFE-wrapped conductive thread. b) Optical images of plain woven or knitted two-in-one triboelectric textiles. c) Open-circuit voltage of the corresponding triboelectric textiles. d) Short-circuit current of the corresponding triboelectric textiles.

of sample Weave 2 is comparatively less dense, with 9 weft segments (2 in. in length) and 30 warp (0.5 in. in length) threads.

Figure 5c,d shows the measured open-circuit voltage and short-circuit currents for the three two-in-one triboelectric textiles. The triboelectric textile sample Weave 1 was tight woven and, therefore, provided minimal power output with stretching. However, gentle patting of the textile with one hand generates power, as shown in Figure 4c,d (Weave 1 pat). The measurement of sample Weave 2 was conducted by either gently stretching the triboelectric textile, as shown in the Video S3 provided in the Supporting Information, or patting the triboelectric textile. The results are shown in Figure 4c,d (Weave 2 stretch and Weave 2 pat).

To increase the effective surface and contact area of the triboelectric textile, a knitted structure, Knit 1, was investigated as shown in Figure 5b. In the knitted structure, the two different threads are closely contacted in parallel throughout the entire textile, and knots provide additional friction sites for multiple threads, as highlighted by the dots in the schematic illustration provided in Figure 5b. The porous structure of the knitted sample should provide ample interthread spacing to achieve larger displacement, which, in theory, should lead to greater charge transfer between the two electrodes and larger short circuit currents.

The sample areas of the triboelectric textiles used for electric output measurements were 1×2 in.^{2} for sample Weave 1, 0.5×2 in.^{2} for sample Weave 2, and 1×2 in.^{2} for sample Knit 1. Sample Weave 1 generated a comparatively erratic V_{oc} that varied between 0.5 and 1 V with hand patting. Sample Weave 2 and sample Knit 1 generated a stable V_{oc} of about 1 V with stretching. Gentle patting on sample Weave 2 generated a V_{oc} of about 3 V. The J_{sc} was 0.014 μA cm^{-2} for sample Weave 1, 0.017 μA cm^{-2} for sample Knit 1, and 0.06 and 0.12 μA cm^{-2} for sample Weave 2 with stretching and with patting, respectively. Among these three triboelectric textiles, Weave 2 yielded the best power output per area. However, it is worth noting that sample Knit 1 had a much smaller density of contact points compared to Weave 1 and Weave 2. Therefore, the correct balance of ample interthread spacing and density of contact points is necessary to optimize the triboelectric power output of two-in-one triboelectric textiles.

Overall, these results indicate that both knitting and weaving methods can be successfully applied to fabricate two-in-one triboelectric textiles. The density of contact points between negative and positive triboelectric materials plays an important role in the power output of the textile. High weave densities only allow for small thread displacements and result in unstable power output, whereas highly porous textiles with few contact points yield low currents and low areal power outputs. Higher electric output can be achieved by both optimizing the knitting or weaving density and varying the weave pattern beyond the single knit or plain woven structures investigated in this work, to realize the most efficient friction and charge collection.

The sewn TEG with face-to-face nylon and functionalized cotton cloths produced an average areal power output of 7 μW cm^{-2}. The two-in-one triboelectric textile Weave 1 provided an areal power output of 0.014 μW cm^{-2} (low estimates, not champion values), while operating under stretching mode. Sample Weave 2 provided an areal power output of 0.06 and 0.36 μW cm^{-2} under stretching and patting mode, respectively. Knit 1 provided an areal power output of 0.017 μW cm^{-2} under stretching mode. The all-textile TEGs reported herein are notable for being one of few functional triboelectric generators constructed using simple textile and garment manufacturing processes, such as sewing, weaving, and knitting. Large-area versions of the lab-scale devices reported herein can be easily assembled using existing textile and garment manufacturing facilities. Therefore, many practical consumer applications can be envisioned for the all-textile TEGs reported herein. For example, if the triboelectric textile Knit 1 were to be used as a window curtain for a standard single pane window, which is typically 24 square feet in area, a maximum power output of 8 mW can be achieved upon gentle stretching of the curtain, which is sufficient to charge many low-power consumer electronic devices. Further, a higher power output than the values reported herein can be achieved if the sewn textile TEG is patched into specific regions of garments, such as in the elbow part of a sleeve, where larger body motion forces are exerted, compared to the gentle stretching and hand patting forces used in these studies. In summary, the strategies described herein to assemble functional, all-textile triboelectric generators will enable seamless integration of triboelectric power harvesting devices into garments and household furnishings, thus providing unexpected options to charge low-power electronics without using energy derived from burning fossil fuels.

3. Conclusion

Two different approaches for creating all-textile TEGs were investigated. The first approach involved sewing together two different cloths of opposite triboelectric properties in a face-to-face configuration. Simple cotton cloths were transformed into negative triboelectric materials via efficient surface functionalization with a polymeric fluoroalkylated siloxane. These functionalized cotton textiles subsequently served as the negative triboelectric material in an all-textile TEG, while nylon cloths were used as the positive triboelectric material. A five-fold V_{oc} increase, threefold J_{sc}, and threefold transferred charge increase was observed in sewn TEGs containing functionalized cotton cloths, as compared to sewn TEGs containing pristine cotton. The enhanced electric output was attributed to an increased surface charge density allowed by the siloxane functionalization, which was confirmed by KPFM measurements. The second approach involved the weaving or knitting together of two different types of conductive threads to create a swatch of a two-in-one triboelectric textile. Both weaving and knitting methods produced functioning triboelectric textiles. The density of contact points between negative and positive triboelectric threads played an important role in the power output of the final textile.

4. Experimental Section

Cotton and nylon textiles were purchased from Dharma Trading Co. Silver/nylon textile was purchased from LessEMF. All textiles were sonicated in water for 15 min prior to use. For surface grafting, cotton textiles were soaked in trichloro(1*H*,1*H*,2*H*,2*H*-perfluorooctyl)silane/hexane (1:100 V/V) for 12 h under air, followed by rinsing in hexane and

drying in air. XPS measurements were conducted on a Thermo Scientific K-alpha instrument. SEM measurements were performed on a Zeiss Leo 1530 field-emission microscope. The topography and surface potential were measured using an AFM Agilent 5500. The average CPD values were obtained by Statistical Quantities function of software Gwyddion. The voltage outputs were recorded using an Agilent DSO1012A oscilloscope. The current outputs and charge transfer amount of TENGs were measured using an Autolab PGSTAT302N station. The external load for all measurements except for the load matching tests was 10 MΩ. For the face-to-face TEG device measurements, the force was 6N on a 1×1 in.^{2} sample, and the speed was 10 mm s^{-1}.

Supporting Information

Supporting Information is available from the Wiley Online Library or from the author.

Acknowledgements

The authors gratefully acknowledge financial support from the US Air Force Office of Scientific Research, under Agreement number FA9550-14-1-0128. T.L.A. also gratefully acknowledges partial support by the David and Lucille Packard Foundation.

Received: July 12, 2016
Revised: September 4, 2016
Published online:

[1] D. J. Norris, E. S. Aydil, *Science* **2012**, *338*, 625.
[2] V. Nico, E. Boco, R. Frizzell, J. Punch, *Appl. Phys. Lett.* **2016**, *108*, 013902.
[3] T. J. Hendricks, S. Yee, S. LeBlanc, *J. Electron. Mater.* **2015**, *45*, 1751.
[4] M. Ha, J. Park, Y. Lee, H. Ko, *ACS Nano* **2015**, *9*, 3421.
[5] Z. L. Wang, *ACS Nano* **2013**, *7*, 9533.
[6] J. Zhong, Y. Zhang, Q. Zhong, Q. Hu, B. Hu, Z. L. Wang, J. Zhou, *ACS Nano* **2014**, *8*, 6273.
[7] L. S. McCarty, G. M. Whitesides, *Angew. Chem., Int. Ed.* **2008**, *47*, 2188.
[8] C. Liu, A. J. Bard, *Nat. Mater.* **2008**, *7*, 505.
[9] S. Niu, S. Wang, L. Lin, Y. Liu, Y. S. Zhou, Y. Hu, Z. L. Wang, *Energy Environ. Sci.* **2013**, *6*, 3576.
[10] F.-R. Fan, L. Lin, G. Zhu, W. Wu, R. Zhang, Z. L. Wang, *Nano Lett.* **2012**, *12*, 3109.
[11] W. Seung, M. K. Gupta, K. Y. Lee, K.-S. Shin, J.-H. Lee, T. Y. Kim, S. Kim, J. Lin, J. H. Kim, S.-W. Kim, *ACS Nano* **2015**, *9*, 3501.
[12] H. Y. Li, L. Su, S. Y. Kuang, C. F. Pan, G. Zhu, Z. L. Wang, *Adv. Funct. Mater.* **2015**, *25*, 5691.
[13] G. Cheng, Z.-H. Lin, L. Lin, Z.-l. Du, Z. L. Wang, *ACS Nano* **2013**, *7*, 7383.
[14] S. Jung, J. Lee, T. Hyeon, M. Lee, D.-H. Kim, *Adv. Mater.* **2014**, *26*, 6329.
[15] S. Lee, W. Ko, Y. Oh, J. Lee, G. Baek, Y. Lee, J. Sohn, S. Cha, J. Kim, J. Park, J. Hong, *Nano Energy* **2015**, *12*, 410.
[16] W. Seung, M. K. Gupta, K. Y. Lee, K.-S. Shin, J.-H. Lee, T. Y. Kim, S. Kim, J. Lin, J. H. Kim, S.-W. Kim, *ACS Nano* **2015**, *9*, 3501.
[17] K. N. Kim, J. Chun, J. W. Kim, K. Y. Lee, J.-U. Park, S.-W. Kim, Z. L. Wang, J. M. Baik, *ACS Nano* **2015**, *9*, 6394.
[18] X. Pu, L. Li, H. Song, C. Du, Z. Zhao, C. Jiang, G. Cao, W. Hu, Z. L. Wang, *Adv. Mater.* **2015**, *27*, 2472.
[19] T. Zhou, C. Zhang, C. B. Han, F. R. Fan, W. Tang, Z. L. Wang, *ACS Appl. Mater. Interfaces* **2014**, *6*, 14695.
[20] Z. Zhao, X. Pu, C. Du, L. Li, C. Jiang, W. Hu, Z. L. Wang, *ACS Nano* **2016**, *10*, 1780.
[21] D. K. Aswal, S. Lenfant, D. Guerin, J. V. Yakhmi, D. Vuillaume, *Anal. Chim. Acta* **2006**, *568*, 84.
[22] C. A. Rezende, R. F. Gouveia, M. A. da Silva, F. Galembeck, *J. Phys.: Condens. Matter* **2009**, *21*, 263002.
[23] J. Molina, M. F. Esteves, J. Fernández, J. Bonastre, F. Cases, *Eur. Polym. J.* **2011**, *47*, 2003.